Journal of Organometallic Chemistry 693 (2008) 3245–3255

Contents lists available at ScienceDirect

Journal of Organometallic Chemistry

journal homepage: www.elsevier.com/locate/jorganchem

Synthesis, characterization, and steric hindrance comparisons of selected transition and main group metal β-ketoiminato complexes

Leslie A. Lesikar, Audra F. Gushwa, Anne F. Richards *

Department of Chemistry, Texas Christian University, Box 298860, Fort Worth, TX 76129, United States

ARTICLE INFO

Article history:
Received 17 June 2008
Received in revised form 15 July 2008
Accepted 17 July 2008
Available online 24 July 2008

Keywords:
Ketoiminato ligands
X-ray crystal structures

ABSTRACT

The coordination preference of the ketoiminato ligand, $RN(H)(C(Me))_2C(Me)=O$, (R = 2,6-diisopropylphenyl, (Dipp)), L^1, and $RN(H)C(Me)CHC(Me)=O$, $R = C_2H_4NEt_2$, L^2, have been investigated with a range of d and p block metal halides, (or alkyls), to compare and contrast products obtained from the bulky ketoiminato ligand, L^1, versus the less bulky, but multidentate ligand, L^2. The products have been characterized by X-ray crystallography along with other spectroscopic techniques and show how the preferred metal geometry remains constant for products with either ligand, but the steric protection offered by the individual ligands governs the nuclearity of the products, affording monomers, dimers and tetramers.

1. Introduction

The chemistry of β-diketoiminato ligands ($[\{N(Ar)C(Me)\}_2CH]^-$, nacnac) has been vastly researched and they have been used to support virtually all elements in the periodic table, many in very low oxidation states [1]. Related to β-diketoiminato ligands are ketoiminato ligands, $RN(H)(C(Me))_2C(Me)=O$, (R = aryl) = L^1. These bidentate ligands with a bulky substituent on one side can protect the metal center while keeping the other side open to increase activity of the metal complexes. Structurally related to nacnac and ligand L^1 is L^2, $RN(H)C(Me)CHC(Me)=O$, $R = C_2H_4NEt_2$, Fig. 1, which features a pendant arm on the nitrogen atom. The pendant arm is postulated to be advantageous as it can tether and protect metal centers because of the NNO tridentate system which can overcome problems associated with the single sided support of ketoiminato ligands.

Other advantages of these ligands are their facile high yielding syntheses, strong coordination ability to metal centers as monovalent and divalent ligands, and steric effects afforded by the substituent on the nitrogen atom. It is well known that β-diketoiminato and β-ketoiminato ligands with bulky substituents have stronger π bonding tendencies to the same acceptor than Schiff-base ligands, and the coordination ability of ketoiminato ligands shows a behavior between that of Schiff-base (NO ligands) and β-diketoiminato N–N ligands, Fig. 2 [2].

Given the wide range of documented nacnac complexes [1], we were interested in the coordination chemistry of L^1 and L^2, in particular comparing the reaction outcome of the relatively bulky RNO ligand, L^1, (R = aryl) compared to the more flexible, but multidentate ligand, L^2. Rather than selecting a particular periodic group to study, we wished to examine the coordination preferences of the ligand, along with how preferred metal geometry affects the product outcome. To this end, reactivity was examined with both d and p block elements. In particular, we wished to target elements that have proven successful with nacnac and have garnered useful biological or technological applications [3]. Herein we compare and contrast the coordination preferences of L^1 and L^2 with $TiCl_2$, $MnCl_2$, Et_2Zn, $InCl_3$ and $SbCl_3$ affording products ranging from tetrameric cages to simple adducts.

2. Results and discussion

2.1. Discussion of the titanium dimer, *1*, and tetramer, *2*

The reaction of lithiated L^1 and L^2 with $TiCl_2$ afforded orange crystals of complexes **1** and **2** in low to moderate yields, respectively, Scheme 1.

As can be seen in Fig. 3, single crystal X-ray analysis of complex **1** revealed a titanium dimer, placed around a center of symmetry, with two ligands coordinated to each metal center and the titanium atoms linked by a bridged oxygen atom, O3. The di-μ-oxo-dititanium ring is planar and slightly distorted from a square, the angles at oxygen being 96.84(9)°.

The product from the reaction of L^2Li with $TiCl_2$ is a tetrameric molecular square supported by one ligand on each metal center, Fig. 4. The presence of trace moisture led to the formation of both complexes **1** and **2**, but the formation of a dimer, **1**, or a tetramer, **2**, was ostensibly governed by the relative steric protection of the ligands. Bidentate ligand L^1 was incapable of providing full

* Corresponding author. Tel.: +1 18172576220; fax: +1 18172575851.
E-mail address: a.richards@tcu.edu (A.F. Richards).

0022-328X/$ - see front matter © 2008 Elsevier B.V. All rights reserved.
doi:10.1016/j.jorganchem.2008.07.021

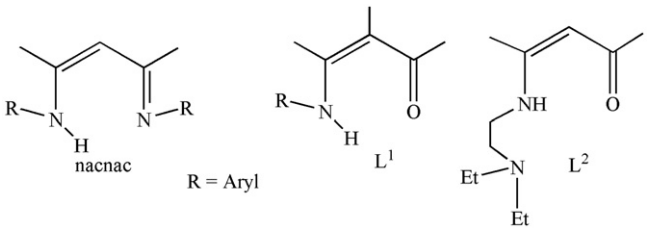

Fig. 1. Chemical representation of the β-diketoiminato (nacnac), ketoiminato, L^1, and the multidentate, RN(H)C(Me)CHC(Me)=O, R = $C_2H_4NEt_2$, L^2, ligands.

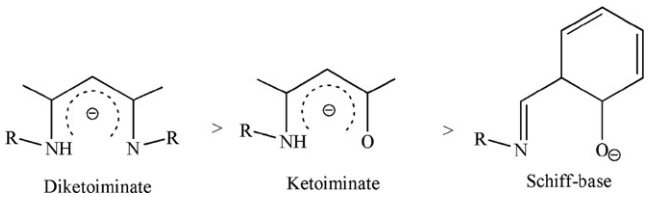

Fig. 2. Coordination ability of the ligands.

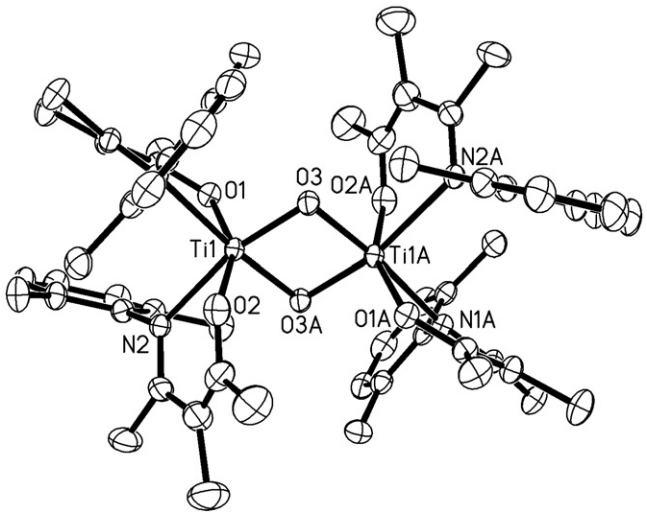

Fig. 3. Molecular structure of 1, hydrogen atoms and a molecule of thf are omitted for clarity. Ti1–O1 1.921(2), Ti1–O2 1.911(2), Ti1–O3 1.835(2), Ti1–N1 2.265(2), Ti1–N2 2.300(3), C1–O1 1.302(4), Ti1–Ti1A 2.7527(10), O3–Ti1–O2 96.01(10), O3–Ti1–O1 103.36(9), O1–Ti1–N1 78.98(8), Ti1–O3–Ti1A 96.84(9). Symmetry transformations used to generate equivalent atoms: $-x, -y-1, -z$.

protection of each Ti center in complex **1**, leaving each metal atom open to coordination by an additional ligand. Conversely, tridentate L^2 forms three contacts with each titanium atom and therefore further protects each Ti center making only one ligand per metal necessary. Nevertheless, the increased flexibility and decreased bulkiness of the pendant arm of L^2 relative to the aryl group of L^1 allowed the Ti center to have sufficient space to increase the O–Ti–O angle of **2** to 98.63(11)° compared to that of 83.16(9)° for **1**. This larger O–Ti–O angle enabled the formation of the tetramer, rather than the four-membered ring of dimer **1**.

During the course of the reaction, Ti^{2+} is oxidized to Ti^{4+} concomitant with the reduction of Ti^{2+} to Ti(0). The point of oxygen contamination was observable by a color change from deep blue-green to brown. In both **1** and **2**, the titanium centers have slightly distorted octahedral geometry. Pertinent bond lengths and angles are given in Figs. 3 and 4. In the dimer, **1**, the distance between the non-bonding titanium centers is 2.7527(10) Å which can be compared to the Ti–Ti distance in bulk titanium of 2.896 Å [4], and to related systems [5] such as [TiO(acac)$_2$] with a Ti–Ti separation of 2.729(1) Å [6]. The dimensions within tetramer **2** are ~3.6 Å from Ti to Ti, which compares well to related systems[7] such as ammonium tetrakis((μ_2-oxo)-bis(oxalato-O,O')-titanium) tetrahydrate that has a Ti–Ti separation of ~3.5 Å [8]. Like the related tetramers, the titanium atoms do not reside in the same plane, resulting in a skewed arrangement in which the chloride atoms on each adjacent titanium adopt 'trans' geometry and ligand repulsion is minimized. Infrared spectroscopy shows characteristic CO and CN stretching bands at 1560 and 1609 cm^{-1} (complex **1**) and at 1527 and 1615 cm^{-1} (complex **2**). A weak signal in the infrared spectrum of **1** at 763 cm^{-1} corresponds well with the ν(Ti–O–Ti) bands at 753 and 754 cm^{-1} reported for the clusters [Ti_6O_6(OSi(CH$_3$)$_3$)$_6$(OOCR)$_6$] (R = Bu^t, Bu^{t}CH$_2$, C(CH$_3$)$_2$Et) [9a] and also with

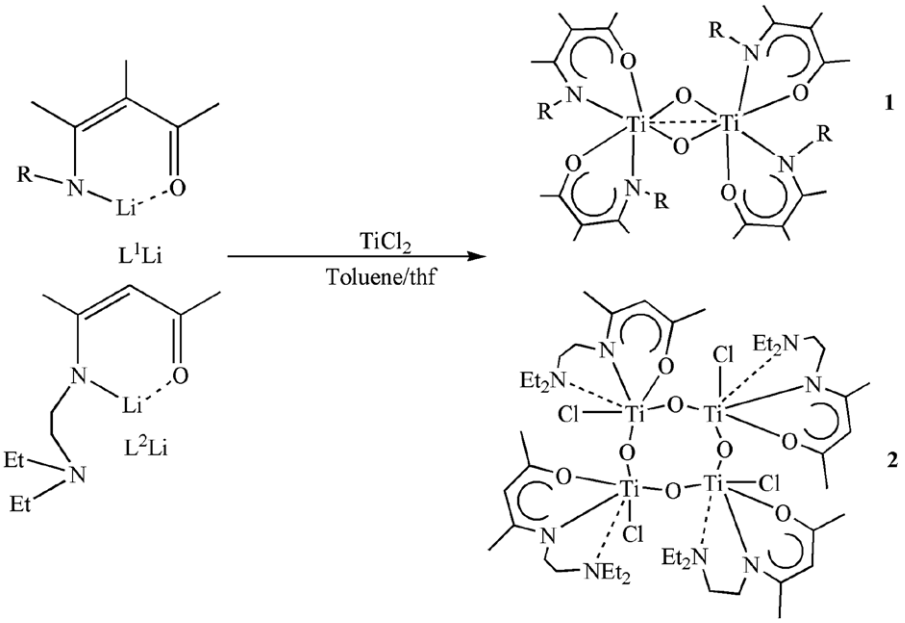

Scheme 1. Synthesis of the titanium dimer, **1** and tetramer, **2**, (R = Dmp (dimethylphenyl).

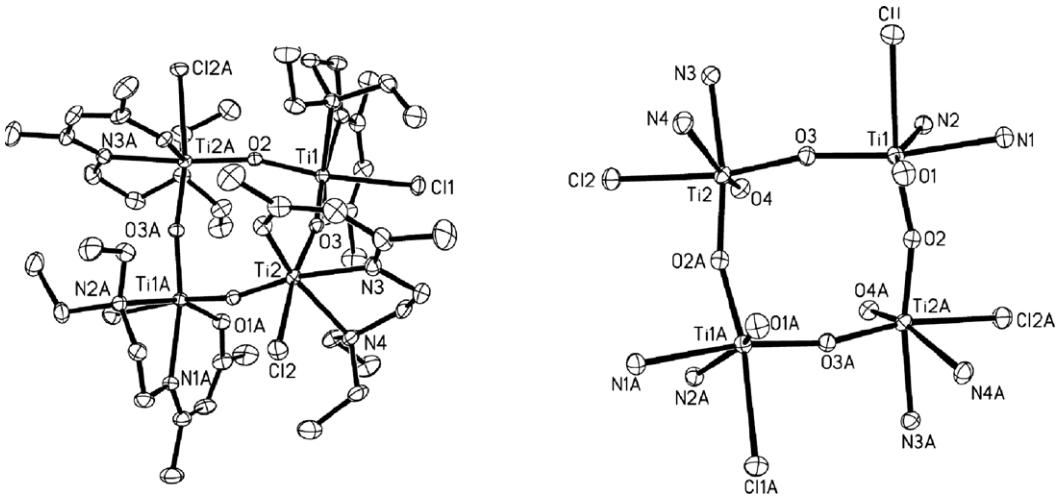

Fig. 4. Molecular structure of complex **2**. Thermal ellipsoids at 30% probability level, hydrogen atoms and two thf molecules are omitted for clarity. Selected bond lengths (Å) and angles (°): Ti1–O1 1.902(3), Ti1–O2 1.830(2), Ti1–O3 1.827(2), Ti1–N1 2.207(3), Ti1–N2 2.300(3), Ti1–Cl1 2.4720(11), Ti1–N2 2.300(3), Ti2–O4 1.899(3), Ti2–N3 2.201(3), Ti2–N4 2.308(3), C1–O1 1.308(5), O3–Ti1–N2 98.47(11), Ti1–O3–Ti2 167.43(15), Cl1–Ti1–O2 170.58(9), O3–Ti1–N1 170.17(12). Symmetry transformations used to generate equivalent atoms: $-x, y, -z+½$.

the analogous signal observed at 762 cm^{-1} in [{η^5-$C_5H_2(SiMe_3)_3$}$_2$-$Ti_2Cl_4(\mu$-O)] [9b]. A similar signal due to Ti–O–Ti vibrations was not observed for **2**. Complexes **1** and **2** are both orange solids and exhibit similar absorption maxima; 220 and 324 nm for **1** and 230 and 304 nm for **2**, which can be attributed to charge transfer to the Ti center.

2.2. Discussion of the manganese complexes [(L^1)$_2$MnCl], 3, and [L^2MnCl · LiCl(thf)$_2$], 4

In keeping with our original goal of targeting specific elements, manganese coordination chemistry has become increasingly interesting [10,11], stemming from the involvement of Mn in several biological redox active systems. Of particular interest is the oxygen evolving complex of photosystem II which is believed to be a tetranuclear Mn aggregate with NO donors [10]. The stoichiometric, room temperature reaction of L^1Li with $MnCl_2$, Scheme 2, afforded the monomeric Mn(III) complex, [$(RNO)_2$MnCl], **3**, in moderate yield, Fig. 5.

Hundreds of Mn–Cl structures have been reported in the literature many of which feature NOMn coordination [12]. The crystal structure of **3** does not display any exceptional differences, although the Mn–Cl bond is fairly short when compared to other Mn(III)Cl systems. For example, Mn(salpn)Cl · MeOH, has a Mn–Cl bond length of 2.493(1) Å [13], (salpn = dichloro-(*N*,*N*'-(salicy1idene)-1,3-propanediamino), however, the majority of these systems feature manganese in an octahedral coordination environment. Crystals of **3**, were originally obtained from the reaction performed at room temperature. To determine whether oxidation of Mn(II) to Mn(III) was occurring because of these reaction conditions, the reaction was repeated at −78 °C and the solution maintained at low temperature in an attempt to slow the reaction down. Under these conditions, complex **3** was isolated.

Adopting similar conditions for the synthesis of **3**, the reaction of L^2Li with $MnCl_2$ afforded complex **4**, a monomeric Mn^{2+} complex in high yield, Fig. 6.

Due to employing the lithiated salt as the reactant, crystallographic analysis revealed incorporation of LiCl in the final product; a common occurrence in transition metal chemistry [14]. In both **3** and **4** the manganese atoms adopt five coordinate, trigonal bipyramidal geometry, with Mn–Cl bonds in **4** of 2.3703(9) Å and 2.4533(9) Å which are comparable to related Mn–Cl systems. The latter, longer, Mn–Cl distance is associated with the bridged Cl, coordinated to the Li center. The UV–Vis of **3** and **4** are characteristic of the different oxidation states of the manganese complexes. For example, the maximum observed at 321 nm for complex **3** can be compared to λ_{max} from three (pyrrolidine salen)Mn(III) complexes (also of the formula [$(RNO)_2$MnCl]): 322, 324, 328 nm [15a]. By comparison the UV–Vis spectrum of **4** displays λ_{max} at 230 and 310 nm that compares well to the corresponding manganese(II) β-diketoiminato complex values of 231 and 376 nm [15b]. The significantly high ε value of 17 400 is indicative of a charge transfer transition [16,17].

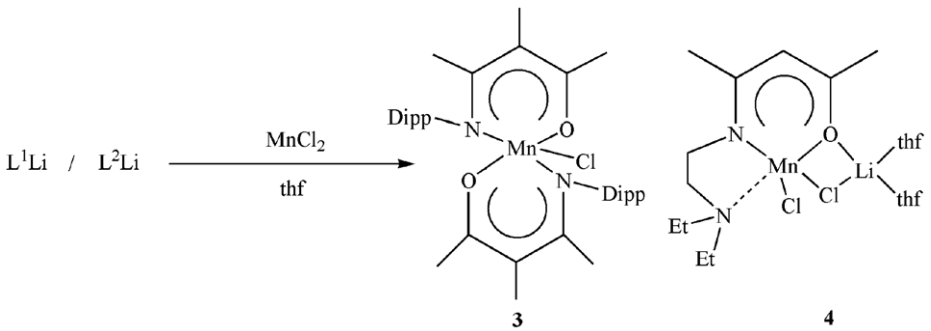

Scheme 2. Synthesis of [(L^1)$_2$MnCl], **3**, and [L^2MnCl·LiCl(thf)$_2$], **4**.

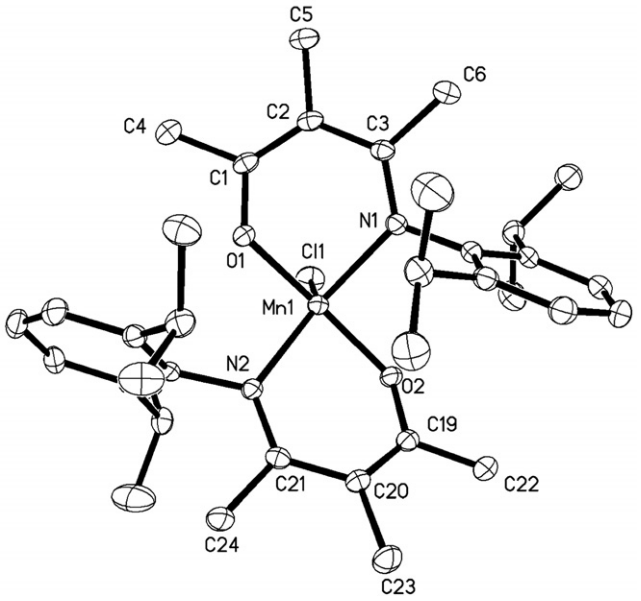

Fig. 5. X-ray crystal structure of $[(L^1)_2MnCl]$, **3**. Thermal ellipsoids at 30% probability level, hydrogen atoms are omitted for clarity. Selected bond lengths (Å) and angles (°): Mn1–O1 1.846(2), Mn1–O2 1.859(2), Mn1–N1 2.071(2), Mn1–N2 2.054(2), Mn1–Cl1 2.3431(10), C1–O1 1.309(3), N1–C3 1.321(4), C2–C3 1.434(4), C1–C2 1.370(4), C19–O2 1.312(2), O1–Mn1–O2 172.94(9), O1–Mn1–N2 88.15(9), O1–Mn1–N1 86.43(9), N2–Mn1–N1 136.41(10).

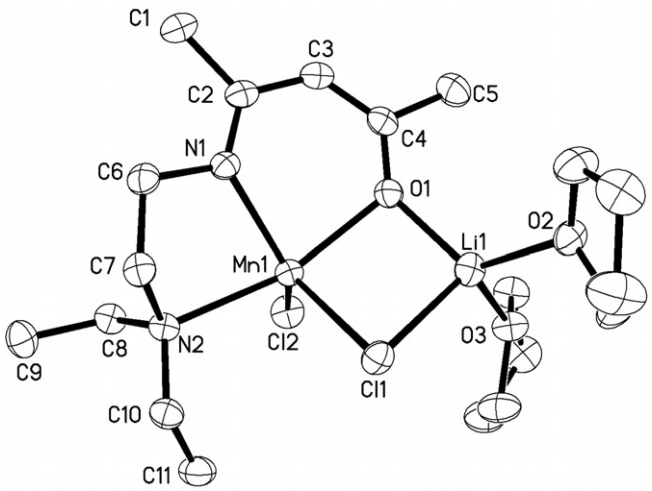

Fig. 6. Molecular structure of **4**, $[L^2MnCl \cdot LiCl(thf)_2]$. Thermal ellipsoids at 30% probability level, hydrogen atoms are omitted for clarity. Selected bond lengths (Å) and angles (°): Mn1–O1 2.144(2), Mn1–N1 2.154(2), Mn1–N2 2.337(2), Mn1–Cl1 2.4533(9), Mn1–Cl2 2.3703(9), Cl1–Li1 2.398(5), Li1–O1 1.895(6), C4–O1 1.294(4), N1–C2 1.306(4), C2–C3 1.428(4), C3–C4 1.360(5), O1–Mn1–N1 83.53(8), O1–Mn1–N2 159.00(8), N1–Mn1–N2 77.95(9), O1–Mn1–Cl1 85.47(6).

2.3. Discussion of the reaction of L^1 and L^2 with $ZnEt_2$

Moving right across the periodic table, the reactions of L^1 and L^2 with diethyl zinc were performed, Scheme 3. β-Diketoiminato complexes with zinc [16] have been studied extensively for their catalytic ability and this has been extended to ketoiminato ligands [19]. Previous work by Liu et al. studied the reaction of L′, that is similar to L^1 except has a hydrogen atom in the γ position, as a potential catalyst for the copolymerization of CO_2 and cyclohexene oxide [20]. No structural analysis of the zinc complexes were performed but the postulated product from the 1:1 reaction of L′ with $ZnEt_2$ was L′ZnEt. We had predicted a similar product for the reaction of L^1 and $ZnEt_2$, yet even in the presence of excess Et_2Zn, the heteroleptic product, L^1ZnEt, could not be obtained and complex **5**, Fig. 7, was isolated, albeit in less yield.

Colorless crystals of complexes **5** and **6** were obtained in moderate yield. Structural analysis revealed that in both complexes, the zinc atom is able to achieve a coordination number of four giving rise to distorted tetrahedral geometry around the zinc center. Complex **5** crystallizes in the monoclinic space group C_2/c and is a homoleptic zinc complex which shows structural resemblance to the related Mg species formed from the reaction of L^1 with $MgBu_2$ [21]. To minimize repulsion between the aryl groups of the ligands they adopt an alternate geometry, which is similarly observed in complex **6**.

In complex **5** the η^2 ketoiminato ligands coordinate to the Zn center with a bite angle of 93.76(5)° which is smaller than regular tetrahedral geometry, (109.28°). The bond lengths within the ligand back bone O1–C1, C–C and C–N are in the range 1.293(2)–1.436(2) Å reflecting partial double bonds in the zinc heterocycle. Like in the related Mg system [21], the two nitrogen atoms of the ketoiminato ligands lie in the horizontal plane.

Complex **6** crystallizes in the tetragonal space group $I\bar{4}$. As has been previously observed in reactions of nacnac [22], ligand rearrangement has occurred, which is believed to arise from the presence of additional donor atoms that become involved in intramolecular coordination affording complex structures. The solid-state analysis revealed four Zn^{2+} cations that occupy the corners of a molecular square or wheel with each ligand acting as a bridge between the metal centers to form an edge. Within the asymmetric unit of **6** are one Zn^{2+} and one molecule of rearranged ligand. An ethyl group retained on the zinc atom balances the cationic charge along with a −1 charge associated with the ligand. Two nitrogen atoms and a dative oxygen interaction occupy the remaining tetrahedral coordination sites around each zinc atom. Examination of the bond lengths and angles in **6** suggests delocalization of the negative charge over the ligand backbone. The Zn–O bonds are within normal values 2.028(5)–2.076(6) Å [23], and correspond to dative bonds [24,25]. The Zn–N bonds vary from 2.19(2)–2.25(2) Å and are comparable to reported Zn–N bonds [18,19]. The solid-state analysis is confirmed by solution NMR where the ^1H NMR spectrum exhibits an indicative single peak associated with the C–H on the backbone at 4.89 ppm. This value can be similarly compared to a slightly downfield C–H backbone shift of 5.45 ppm that was observed in a related zinc β-ketoiminato complex where a macrocycle structure of six units formed [26]. The IR bands of **6** are also similar to those previously reported [17–19] occurring at 1585 (C=O), 1509 (C=C), and 1412 cm^{-1} (C–N) (see Fig. 8).

The tetrameric outcome of the reaction of L^2 with $ZnEt_2$ is not too surprising given that zinc alkoxides readily give rise to zinc tetramers that often feature a distorted cubic Zn_4O_4 [25]. The degree of association is dependent on ligand size and decreases with increasing bulk resulting in dimers, trimers or monomers [27,28]. Thus, the bulkier ligand, L^1, can stabilize a monomeric species, whereas the less bulky L^2, yields a tetramer. The distances within the core from each zinc atom are ~7.77 Å. These distances can be compared to related documented systems of 11.11 Å or 8.6 Å as observed in the tetramers, $[Zn_4H_8L^1_4][PF_6]_5[NO_3]_3S$ and $[Zn_4H_8L^2_4][PF_6]_6[NO_3]_2 \cdot S$ (L = bistridentate Schiff-base ligands, S = solvent) [29]. Within the tetrameric core are channels that are estimated to be about 494.6 $Å^3$, that correlates to about 14.3% of the crystal volume, calculated by PLATON [30]. The identity of a solvent within the channel could not be resolved by X-ray crystallography and was omitted from the final refinement by SQUEEZE [30]. The unidentified solvent is believed to be a disordered water molecule which was confirmed by spectroscopic techniques [31]. The cause

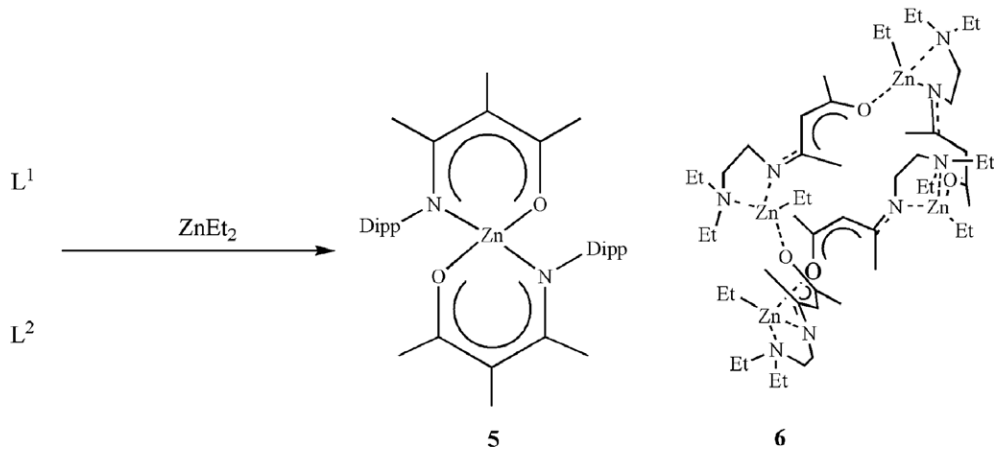

Scheme 3. Reaction products from the reaction of $ZnEt_2$ with L^1 and L^2.

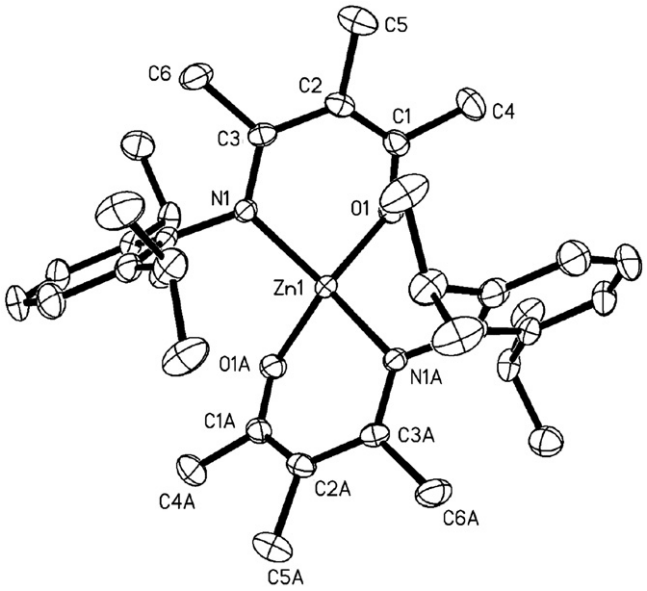

Fig. 7. Crystal structure of the homoleptic zinc complex, **5**. Thermal ellipsoids at 30% probability level, hydrogen atoms are omitted for clarity. Selected bond lengths (Å) and angles (°): Zn1–N1 1.9835(12), Zn1–O1 1.9186(11), C1–O1 1.293(2), N1–C3 1.322(2). C1–C2 1.388(3), C2–C3 1.425(2), N1–Zn1–O1 93.76(5), N1–Zn1–N1A 131.78(8). Symmetry operations used to generate equivalent atoms: $-x+1$, y, $-z+½$.

of water contamination is not confirmed but is most likely from atmospheric water contamination during the reaction, as has been seen with related zinc systems [32]. Attempts to achieve elimination of two ethane molecules through the 2:1 reaction were unsuccessful and resulted in an oily residue. Crystals of **5** and **6** decompose rapidly on exposure to air.

2.4. Indium structures $[(L^1)_2InCl]$, **7** and $[L^2InCl_2]$, **8**

To enable a comparison of coordination preferences of the ligand and metals, main group halides were selected for reaction with L^1 and L^2. There has been increasing interest in organoindium complexes because of their potential use as CVD precursors for the production of III–V and III–VI composite semiconductors [33]. More recently, research has focused on indium complexes supported by oxygen ligands as these are potentially useful for the preparation of In_2O_3 thin films, which are used as transparent conductors in applications such as display panels and solar cell windows [34]. Since homoleptic β-diketonates have been successfully employed for this purpose [35], we deemed that L^1 and L^2 might also prove useful precursors and the reactions of L^1Li and L^2Li with $InCl_3$ were performed, Scheme 4.

The molecular structures of **7** and **8**, Figs. 9 and 10, were determined by X-ray crystallography. In both cases, the indium metal atom adopts distorted trigonal bipyramidal geometry, typical for five coordinate indium derivatives [36]. Continuing the theme of observing similar molecular geometry in the structures obtained from L^1 and L^2, the trend held true for both indium complexes **7** and **8**.

Complex **7** from the reaction of L^1Li with $InCl_3$ at room temperature or low temperature affords an In(III) structure featuring two ligand molecules on one indium center and a terminal halide. Employing analogous reaction conditions for L^2Li the resultant product has one ligand molecule and two terminal halides. The formation of **8** can in part be attributed to the preferred trigonal bipyramidal geometry of the indium atom, and by the presence of the coordinating 'arm', which is able to occupy vacant coordination sites and prevent further ligand coordination. In complex **8** the nitrogen atoms on the pendant arm form a dative bond to the In center, with a In–N bond length of 2.337(3) Å, which is slightly longer than the N → In interaction of 2.466(1) Å in $[In(Me)_2(amak)]_2$ where amak = $HOC(CF_3)CH_2NHR$, R = $(CH_2)_2OMe$, or $Me_2In(C_6H_4CH_2NMe_2)$ of 2.38(1) Å [37]. This bond length is also longer than the sum of the covalent radii, 2.19 Å, of N(sp^3) and O [38]. Complex **8** is structurally similar to that of $[InMe_2(keim)]$ where keimH is a tridentate ketoimine ligand of structural formula $O{=}C(CF_3)CH_2C(CF_3){=}NCH_2CH_2NMe_2$, which also has a long interaction of 2.428(2) Å from the pendant nitrogen atom to the trigonal bipyramidal indium atom [39]. The IR spectra of both **7** and **8** display the characteristic peaks expected [37,39,40].

2.5. Reactions of L^1 and L^2Li with $SbCl_3$

To complete the series, and as a continuation of our earlier work of nacnac-Sb complexes [41], the reactions of the lithiated ligands with $SbCl_3$ were performed, Scheme 5.

Colorless crystals of **9** were obtained from the 1:1 reaction of L^1Li with $SbCl_3$, Scheme 5, Fig. 11. Despite employing the lithiated reagent, no LiCl displacement was observed in the crystallographic analysis, however, **9**, could only be isolated in low yield. The isolation of **9** is most likely from an incomplete lithiation reaction, and indeed a higher yield of product can be obtained from the direct reaction of L^1 with $SbCl_3$. The structural features of **9** are

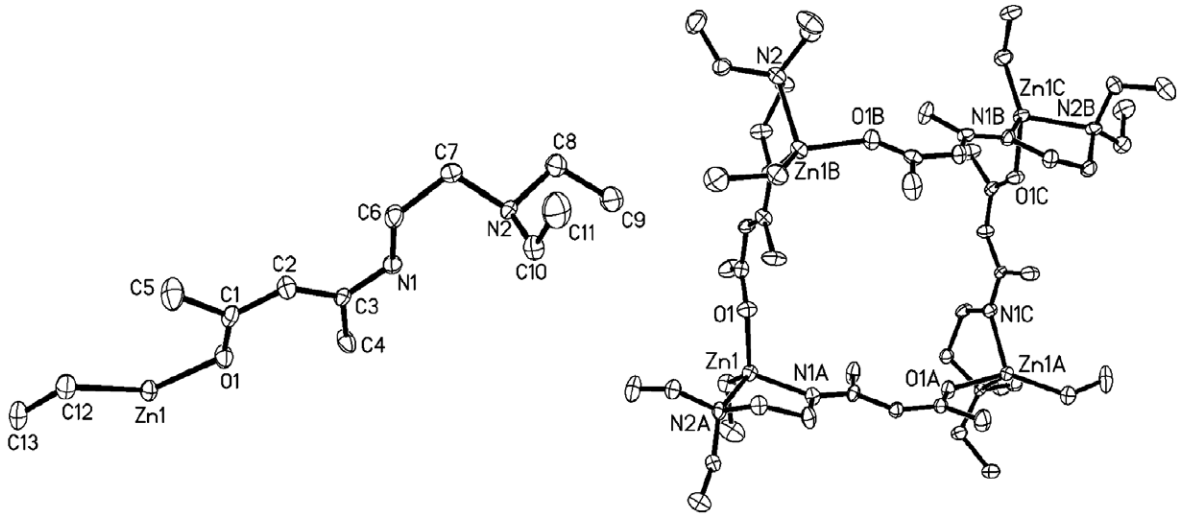

Fig. 8. X-ray crystal structure of **6**. On the left hand side is the asymmetric unit and on the right hand side the tetrameric product is displayed. Thermal ellipsoids at 30% probability level, hydrogen atoms are omitted for clarity. Selected bond lengths (Å) and angles (°): Zn1–O1 2.024(3), N1–C3 1.321(4), N1–C6 1.443(6), N2–C7 1.488(5), C1–O1 1.268(5), C1–C2 1.395(5), C3–C4 1.481(7), C12–Zn1–O1 124.14(17). Symmetry transformations used to generate equivalent atoms: #1 $-y, x-1, -z$, #2 + 1, $-x, -z$.

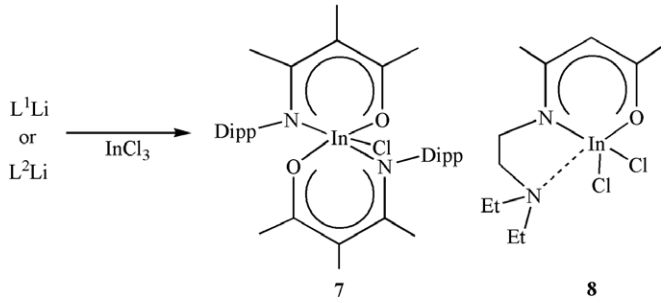

Scheme 4. Synthesis of $[(L^1)_2InCl]$, **7** and $[L^2InCl_2]$, **8**.

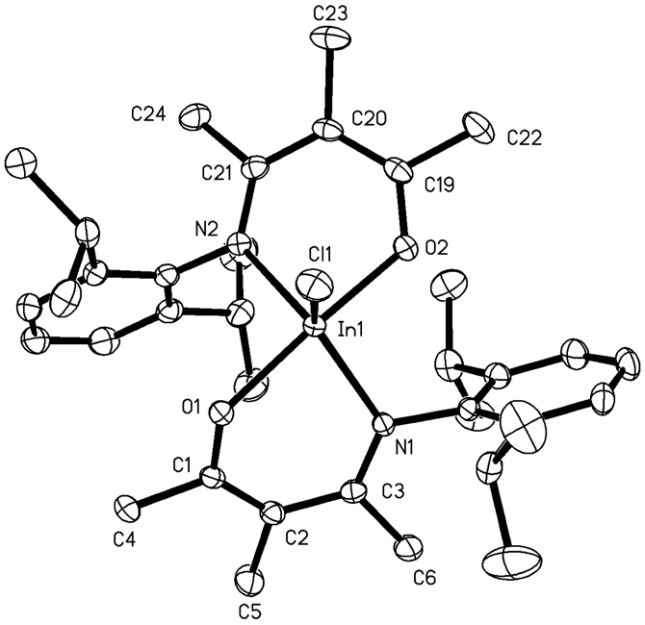

Fig. 9. Crystal structure of **7**, $[(L^1)_2InCl]$. Thermal ellipsoids at 30% probability level, hydrogen atoms are omitted for clarity. Selected bond lengths (Å) and angles (°): In1–O1 2.087(2), In1–O2 2.090(2), In1–N1 2.177(2), In2–Cl1 2.3782(9), C1–O1 1.296(3), N1–C3 1.333(4), C2–C3 1.427(4), C1–C2 1.386(4), C19–O2 1.294(4), O1–In1–O2 167.47(9), O1–In1–N1 83.96(8), O2–In1–N1 88.78(8), N1–In1–N2 127.33(9).

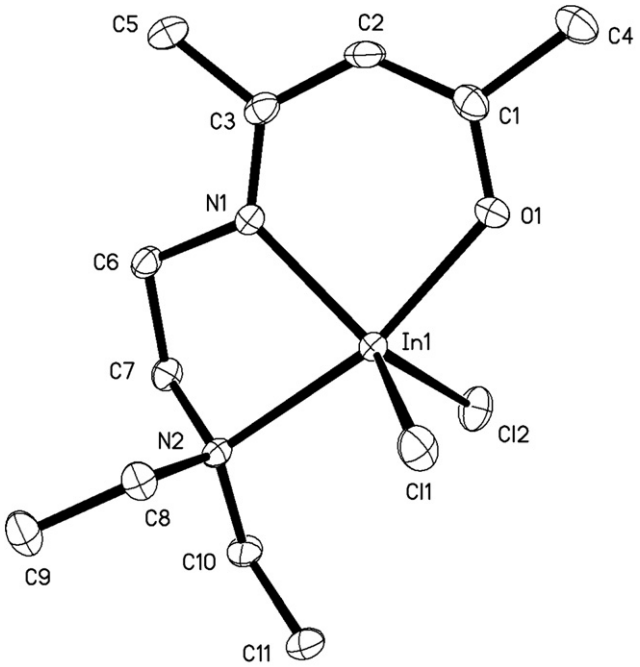

Fig. 10. Crystal structure of **8**, $[L^1InCl_2]$. Thermal ellipsoids at 30% probability level, hydrogen atoms are omitted for clarity. Selected bond lengths (Å) and angles (°): In1–O1 2.119(2), In1–N1 2.152(3), In1–N2 2.337(3), In1–Cl1 2.3810(11), In1–Cl2 2.3812(10), C1–O1 1.288(5), C1–C2 1.373(6), C2–C3 1.419(6), C3–N1 1.331(5), O1–In1–N1 87.64(11), O1–In1–N2 165.92(13), N1–In1–N2 78.31(13), O1–In1–Cl1 91.82(9), O1–In1–Cl2 92.56(9).

unremarkable. The infrared spectra of **9** exhibited a characteristic N–H stretch at 3185 cm^{-1}, which was confirmed by ^1H NMR with a resonance observed at 12.84 ppm [42]. Isolation of the $[L^1SbCl_2]$ product with concomitant loss of LiCl could not be achieved despite the facile syntheses of analogous nacnac-Sb complexes [41].

By contrast, the in-situ lithiation of L^2 and subsequent reaction with $SbCl_3$, yields complex **10**, $[L^2SbCl_2]$, Scheme 5. The geometry around the antimony center is square pyramidal, with the lone pair occupying the vacant site. Spectroscopic data supported the X-ray crystal structure and is unexceptional. Complexes **9** and **10** are air stable, but complex **10** has slightly lower thermal stability.

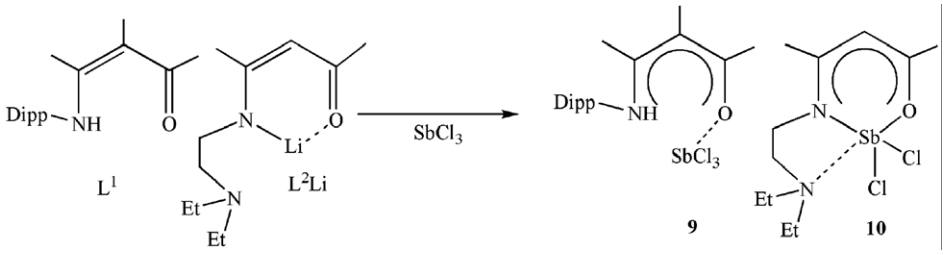

Scheme 5. Synthesis of the antimony complexes **9** and **10**.

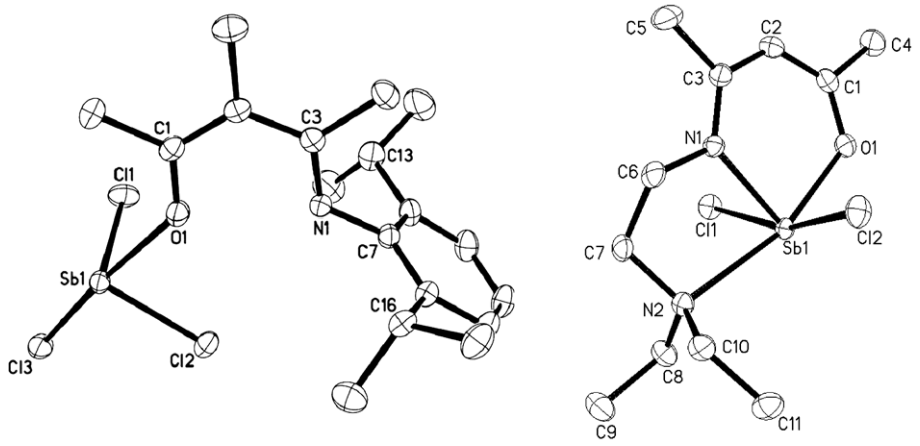

Fig. 11. X-ray crystal structure of [L^1 $SbCl_3$], **9** and [L^2SbCl_2], **10**. Thermal ellipsoids at 30% probability level, hydrogen atoms are omitted for clarity. Selected bond lengths (Å) and angles (°): **9**: Sb1–O1 2.329(2), Sb1– Cl1 2.3494(8), C1–O1 1.296(4), N1–C3 1.327(4), C2–C3 1.416(4), C1–C2 1.394(4), O1–Sb1–Cl3 170.21(6), C3–N1–C7 126.8(3) **10**: Sb1–O1 2.0929(18), Sb1–N1 2.144(2), Sb1–N2 2.481(2), Sb1–Cl1 2.5885(7), C1–O1 1.296(3), C1–C2 1.362(4), C2–C3 1.408(4), N1–C3 1.316(3), O1–Sb1–N1 87.23(8), O1–Sb1–N2 163.26(7), N2–Sb1–Cl2 93.03(5).

3. Conclusion

A series of metal complexes have been prepared using two similar ketoiminato ligands, L^1 and the less bulky, multidentate molecule L^2. The X-ray crystallographic analysis on ten complexes revealed that the preferred metal geometry predominates in the solid-state; however it is the steric preferences of the ligand that govern the nuclearity of the product. These steric differences are

Table 1
Crystal data for compounds **1–5**

Compound name	**1**, $[(L^1_2TiO)_2(thf)]$	**2**, $[(L^2TiOCl)_4(thf)_2]$	**3**, $[(L^1)_2MnCl]$	**4**, $[L^2MnCl{\cdot}LiCl(thf)_2]$	**5**, $[(L^1)_2Zn]$
Chemical formula	$C_{64}H_{88}N_4O_8Ti_2$	$C_{60}H_{114}Cl_4N_8O_{12}Ti_4$	$C_{36}H_{52}MnClN_2O_2$	$C_{19}H_{37}Cl_2LiMnN_2O_3$	$C_{36}H_{52}N_2O_2Zn$
Formula Weight	1137.18	1472.99	635.19	474.29	610.17
Crystal system	Monoclinic	Monoclinic	Triclinic	Monoclinic	Monoclinic
Space group	$P2_1/c$	C_2/c	$P\bar{1}$	$P2_1/n$	C_2/c
Temperature (K)	213(2)	213(2)	213(2)	233(2)	213(2)
a (Å)	12.076(3)	27.416(2)	10.6024(19)	10.1752(16)	21.7773(15)
b (Å)	13.519(3)	12.4262(9)	11.864(2)	12.520(2)	13.7154(9)
c (Å)	21.687(5)	22.3156(16)	15.236(3)	19.603(3)	11.9154(8)
α (°)	90	90	78.842(4)	90	90
β (°)	120.799(11)	103.8440(10)	70.185(3)	104.022(2)	104.5950(10)
γ (°)	90	90	73.316(4)	90	90
V (Å^3)	3041.2(12)	7381.5(9)	1717.2(5)	2422.9(7)	3444.1(4)
Z	2	4	2	4	4
Reflections collected	26194	26699	8431	11885	8215
Independent reflections	7250	8405	6072	4360	3086
Data/restraints/parameter ratio	7250/0/361	8405/14/387	6072/0/392	4360/0/255	3086/0/193
$[R_{(int)}]$	0.0365	0.0428	0.0252	0.0317	0.0197
D_{calc} (mg/m^3)	1.242	1.325	1.228	1.300	1.177
$F(000)$	1216	3128	680	1004	1312
R indices (all data)	$R_1 = 0.0973$, $wR_2 = 0.1986$	$R_1 = 0.0908$, $wR_2 = 0.1870$	$R_1 = 0.0776$, $wR_2 = 0.1246$	$R_1 = 0.0604$, $wR_2 = 0.1312$	$R_1 = 0.0331$, $wR_2 = 0.0779$
Final R indices $[I > 2\alpha(I)]$	$R_1 = 0.0623$, $wR_2 = 0.1713$	$R_1 = 0.0570$, $wR_2 = 0.1550$	$R_1 = 0.0470$, $wR_2 = 0.1065$	$R_1 = 0.0430$, $wR_2 = 0.1102$	$R_1 = 0.0279$, $wR_2 = 0.0731$
Largest difference in peak and hole (e Å^{-3})	1.311 and −0.538	0.989 and −0.607	0.370 and −0.313	0.737 and −0.431	0.251 and −0.150

Table 2
Crystal Data for Compounds 6 – 10

Compound name	**6**, $[(L^2ZnEt)_4]$	**7**, $[(L^1)_2InCl]$	**8**, $[L^2InCl_2]$	**9**, $[L^1SbCl_3]$	**10**, $[L^2SbCl_2]$
Chemical formula	$C_{13}H_{26}N_2OZn$	$C_{36}H_{52}ClInN_2O_2$	$C_{11}H_{21}Cl_2N_2OIn$	$C_{18}H_{27}Cl_3NOSb$	$C_{11}H_{21}Cl_2N_2OSb$
Formula weight	291.73	695.07	383.02	501.51	389.95
Crystal system	Tetragonal	Triclinic	Monoclinic	Triclinic	Monoclinic
Space group	$I\bar{4}$	$P\bar{1}$	C_c	$P\bar{1}$	$P2_1/c$
Temperature (K)	213(2)	213(2)	213(2)	213(2)	213(2)
a (Å)	20.434(3)	10.6732(12)	9.8513(12)	9.4374(8)	10.8864(9)
b (Å)	20.434(3)	11.7261(13)	12.0890(14)	10.2673(9)	11.3392(10)
c (Å)	8.288(3)	15.5111(17)	13.4055(16)	12.2742(11)	13.5520(11)
α (°)	90	89.909(2)	90	95.517(2)	90
β (°)	90	70.975(2)	109.242(2)	94.975(2)	111.5950(10)
γ (°)	90	73.563(2)	90	111.332(2)	90
V (Å^3)	3460.6(14)	1751.4(3)	1507.3(3)	1093.17(17)	1555.5(2)
Z	8	2	4	2	4
Reflections collected	14369	10208	3971	5900	14812
Independent reflections	3112	7732	1936	3899	2810
Data/restraints/parameter ratio	3112/0/160	7732/0/385	1936/2/159	3899/0/224	2810/0/158
$[R_{(int)}]$	0.1147	0.0207	0.0245	0.0317	0.1020
D_{calc} (mg/m^3)	1.120	1.318	1.688	1.524	1.665
$F(000)$	1248	728	768	504	776
R indices (all data)	$R_1 = 0.0649$, $wR_2 = 0.0641$	$R_1 = 0.0559$, $wR_2 = 0.0892$	$R_1 = 0.0204$, $wR_2 = 0.0399$	$R_1 = 0.0335$, $wR_2 = 0.0881$	$R_1 = 0.0312$, $wR_2 = 0.0755$
Final R indices $[I > 2\sigma(I)]$	$R_1 = 0.0441$, $wR_2 = 0.0610$	$R_1 = 0.0386$, $wR_2 = 0.0804$	$R_1 = 0.0186$, $wR_2 = 0.0391$	$R_1 = 0.0319$, $wR_2 = 0.0860$	$R_1 = 0.0280$, $wR_2 = 0.0731$
Largest difference in peak and hole (e Å^{-3})	0.362 and −0.310	0.897 and −0.510	0.279 and −0.317	0.997 and −1.256	0.968 and −0.766

highlighted by the products obtained from the reaction of ligands L^1 and L^2 with $TiCl_2$ and $ZnEt_2$. Employing the ketoiminato ligand, L^1, for titanium yields a bridged oxo dimer; and for zinc, a homoleptic zinc complex. Under similar conditions, reactions of the more flexible, but less bulky, ligand L^2 afforded tetrameric titanium and zinc complexes. Future work will study the further chemistry of the reported structures and will further examine the reactivity of these ligands with main group halides (see Tables 1 and 2).

4. Experimental

All manipulations were performed under anaerobic conditions using standard Schlenk techniques. Toluene was dried using an MBraun-SPS solvent purification system, and thf was dried over potassium before use. The ligands and the corresponding lithium salts were prepared according to literature procedures [43]. All chemicals were purchased from Aldrich and used as received. Crystal data were collected with a Bruker SMART 1000 diffractometer, molybdenum radiation ($\lambda = 0.7107$ Å) at −60 °C. Crystals were mounted on glass fibers using paratone oil. The data were corrected for absorption. Structures were solved by direct methods [44] and refined [44] via full-matrix least squares. The NMR data was recorded on a Varian XL-300, IR analysis was conducted on a MIDAC M4000 Fourier transform infrared (FT IR) spectrometer, UV–Vis absorption spectra were recorded on an Agilent 8453 UV–Vis spectrometer, and mass spectrometry analysis was carried out using a Bruker Esquire 6000 Mass Spectrometer. Melting points were determined in capillaries under a nitrogen atmosphere and are uncorrected.

4.1. Synthesis of **1**, $[(L^1_2TiO)_2(thf)]$

To a Schlenk flask charged with $TiCl_2$ (0.19 g, 1.6 mmol) and L^1Li (0.35 g, 1.6 mmol) was added toluene and thf at room temperature, and stirring was continued overnight. The following day the solvent was removed from the deep blue-green reaction mixture to give a dark blue-green solid. After extraction into thf and filtration, insoluble Ti(0) was observed in the filter flask and the filtrate had changed to an opaque brown color. Storage at room temperature yielded yellow crystals of **1.** Yield: 0.077 g, 18% yield (based on 4:1 ligand to product ratio). M.p. 111–113 °C crystals partially melted, 121–125 °C (decomp.) residue turned red, 144–149 °C residue turned black. IR (Nujol Mull): ν (cm^{-1}) 763 (w), 968 (w), 1560 (m), 1609 (m). UV–Vis (thf, 25 °C): λ (nm) 220, 324. MS (*m/z*; (found (Calc.)): 1137.5 (1137.2) M^+, 1987.3 (1986.0) 2M-4thf, 216.2 (216.3) ligand L^1-H.

4.2. Synthesis of **2**, $[(L^2TiOCl)_4(thf)_2]$

A thf solution of L^2H (0.35 g, 1.8 mmol) was cooled for several minutes at −78 °C, and *n*-BuLi (1.1 mL of a 1.6 M solution in hexanes, 1.8 mmol,) was added drop-wise. After stirring for 5 h at room temperature, the solution of L^2Li was added rapidly by cannula to a thf suspension of $TiCl_2$ (0.32 g, 2.7 mmol) at −78 °C. The resulting cloudy brown reaction mixture was allowed to warm to room temperature gradually and to stir overnight. Filtration of the mixture and storage at room temperature afforded large orange crystals of **2**. Yield: 0.63 g, 65% (based on 4:1 $TiCl_2$ to product ratio). M.p. 108–118 °C (decomp.) orange powder turned to a deep red wax, which did not melt below 250 °C. IR (Nujol Mull): ν (cm^{-1}) 1204 (w), 1527 (w), 1615 (w). UV–Vis (thf, 25 °C): λ (nm) 230, 304. MS (*m/z*; (found (Calc.)): 1137.5 (1137.1).

4.3. Synthesis of **3**, $[(L^1)_2MnCl]$

A thf solution of L^1H (0.5 g, 1.8 mmol) was stirred for several minutes at 0 °C, after which *n*-BuLi (0.73 mL of a 2.5 M solution in hexanes, 1.8 mmol,) was added drop-wise. After stirring an additional 2 h at room temperature, the resultant clear yellow solution was added rapidly via cannula to a suspension of $MnCl_2$ (0.23 g, 1.8 mmol) at room temperature. After 10 min of stirring, the initially cloudy red reaction mixture became clear red and was allowed to stir an additional 2.5 h. The solvent was removed *in vacuo*, yielding a foamy orange solid that was then taken up into a toluene/hexane mix. Following filtration and storage overnight at room temperature, dark red crystals of **3** were obtained. Yield: 0.41 g, 35% yield (based on $MnCl_2$). M.p. 102–103 °C crystals became waxy in appearance, never melted below 250 °C. IR (Nujol Mull): ν (cm^{-1}) 767 (m), 848 (w), 893 (w), 935 (w), 971 (m), 1150 (m), 1304 (s), 1560 (s), 1606 (s). UV–Vis (thf, 25 °C): λ (nm) 321. MS (*m/z*; (found (Calc.)): 457.3 (457.7) M-H_2NDipp, 274.2 (274.4) ligand L^1+H.

4.4. Synthesis of **4**, [$L^2MnCl{\cdot}LiCl(thf)_2$]

To a solution of L^2H (0.50 g, 2.5 mmol) in thf was added 1 equiv. of *n*-BuLi (1.01 mL of a 2.5 M solution, 2.5 mmol) drop-wise at −78 °C. The solution was slowly warmed to room temperature and stirred for 2 h, after which time it was rapidly added to a stirred thf suspension of $MnCl_2$ (0.32 g, 2.5 mmol) at room temperature. The initial cloudy yellow solution gradually turned to a clear golden orange upon stirring for 45 min and stirring was maintained overnight. After concentrating, filtering, and storage at 5 °C overnight, pale yellow chunk crystals of **4** were obtained. Yield: 0.52 g, 43%. M.p. 99–104 °C (decomp.). IR (Nujol Mull): ν (cm^{-1}) 736 (w), 753 (w), 891 (m), 918(m), 939 (m), 1045 (m), 1136 (w), 1155 (w), 1304 (w), 1510 (m), 1595 (m). UV–Vis (CH_2Cl_2, 25 °C): λ (nm) 230, 310. MS (*m/z*; (found (Calc.)): 328.2 (329.8) M−2(thf); 252.1 (252.2) M−2(thf)−LiCl-Cl; 199.1 (198.2) $Et_2NCH_2CH_2N(H)C(Me)CHC(Me)O$.

4.5. Synthesis of **5**, [$(L^1)_2Zn$]

To a stirring hexane solution of L^1H (0.35 g, 1.3 mmol) at −78 °C was slowly added $ZnEt_2$ (1.3 mL of a 1.0 M solution in hexane, 1.3 mmol), resulting in the evolution of a colorless gas. The dry-ice bath was removed after 5 min and the reaction mixture warmed to ambient temperature. Stirring was maintained for 16 h during which time a white precipitate formed. Following filtration of the reaction mixture and storage of the pale yellow filtrate at room temperature, very large colorless crystalline chunks of **5** were obtained. Yield: 0.45 g, 58% (based on $ZnEt_2$). M.p. 122–123 °C crystals became "sweaty," 170–181 °C (decomp.) solid turned yellow, 240–245 °C yellow solid turned red and melted. ^1H NMR ($CDCl_3$, 25 °C): δ (ppm) 1.00 (d, 6H, $CH(CH_3)_2$, $^1J_{H-H}$ = 6.74 Hz), 1.07 (d, 12H, $CH(CH_3)_2$, $^1J_{H-H}$ = 6.74 Hz), 1.11 (d, 6H, $CH(CH_3)_2$, $^1J_{H-H}$ = 7.04 Hz), 1.54 (s, 3H, C*Me*), 1.59 (s, 6H, C*Me*), 1.63 (s, 3H, C*Me*), 1.85 (s, 3H, C*Me*), 2.17 (s, 3H, C*Me*), 2.94 (septet, 4H, $CH(CH_3)_2$, $^1J_{H-H}$ = 6.74 Hz), 7.01 (m, 4H, phenyl C–*H*), 7.20 (d, 2H, phenyl C–*H*, $^1J_{H-H}$ = 3.81 Hz). ^{13}C NMR ($CDCl_3$, 25 °C): δ (ppm) 15.0 ($CH(CH_3)_2$), 16.8 ($CH(CH_3)_2$), 23.0 ($NCCH_3$), 24.7 ($OCCH_3$), 28.7 ($CH(CH_3)_2$), 98.8 (NCCCO), 123.7 (phenyl *C*H), 128.0 (phenyl *C*H), 134.6 (phenyl *C*-*i*Pr), 146.5 (phenyl *C*–N), 161.9 (*C*N), 196.1 (*C*O). IR (Nujol Mull): ν (cm^{-1}) 986 (s), 1055 (m), 1146 (m), 1173 (w), 1204 (w), 1276 (s), 1322 (s), 1505 (m), 1555 (m), 1561 (s). MS (*m/z*; (found (Calc.)): 611.4 (611.2) M+H, 272.0 (272.4) ligand L^1-H.

4.6. Synthesis of **6**, [$(L^2ZnEt)_4$]

$ZnEt_2$ (1.8 mL of a 1.0 M solution in hexane, 1.8 mmol) was added neat to a solution of L^2H (0.35 g, 1.8 mmol) in toluene at room temperature. An immediate color change was observed and the resultant bright yellow reaction mixture was stirred for 3 h. The solvent was then removed *in vacuo* and the yellow solid was extracted into hexane. Concentration of the solution and storage at −30 °C overnight, afforded colorless needles of **6**. Yield: 0.16 g, 30%. M.p. 176–181 °C. ^1H NMR ($CDCl_3$, 25 °C): δ (ppm) 0.97 (t, 9H, $^1J_{H-H}$ = 7.05 Hz, CH_3CH_2Zn, CH_3CH_2N), 1.18 (s, 3H, NC*Me*), 1.87 (s, 2H, H_2O), 1.93 (s, 3H, OC*Me*), 2.45–2.57 (m, 8H, CH_3CH_2N, NCH_2CH_2N), 3.23 (q, 2H, $^1J_{H-H}$ = 6.50 Hz, CH_3CH_2Zn), 4.89 (s, 1H, γ-C*H*). ^{13}C NMR (C_6D_6, 25 °C): δ (ppm) 10.9 (CH_3CH_2Zn), 13.1 (NC*Me*), 18.1 (OC*Me*), 27.8 (CH_3CH_2Zn), 28.7 (CH_3CH_2N), 40.6 (CH_3CH_2N), 46.2 (NCH_2CH_2N), 51.5 (NCH_2CH_2N), 94.2 (γ-CH), 161.7 (*C*N), 193.7 (*C*O). IR (Nujol Mull): ν (cm^{-1}) 938 (m), 1412 (m), 1509 (m), 1585 (m). MS (*m/z*; (found (Calc.)): 309.3 (309.7) M^+; 292 (291.7) M−H_2O; 260.0 (262.6) M−H_2O−Et; 250.1 (251.5) M−2Et; 205.3 (204.5) M−H_2O−3Et; 177.0 (175.7) M−H_2O−Et−Me−NEt_2; 143.0 (142.1) M−3Et−Zn−Me; 122.2 (124.0) M−H_2O−3Et−Zn−Me.

Confirmatory evidence that water is the unresolved solvent molecule in the channels of **6**: ^1H NMR exhibited a distinctive singlet peak at 1.86 ppm, that integrated to two protons. The positive-mode mass spectrum of **6** further confirmed the presence of the water molecule with a peak at *m/z* = 309.3 followed by sequential loss of the water molecule to give a peak at *m/z* = 292 representing the asymmetric unit of **6**.

4.7. Synthesis of **7**, [$(L^1)_2InCl$]

A thf solution of L^1H (0.50 g, 0.1.8 mmol) had 1 equiv. of *n*-BuLi (0.73 mL of a 2.5 M solution, 1.8 mmol) added drop-wise at 0 °C. The solution was allowed to warm to room temperature slowly and stirred for 2 h, after which time it was rapidly added to a stirred thf suspension of $InCl_3$ (0.40 g, 1.8 mmol) at room temperature. The resulting bright yellow solution was allowed to stir overnight, after which time the thf was removed *in vacuo*. The pale orange solid was extracted into toluene (20 mL), filtered, and concentrated until saturated. Overnight storage of the toluene solution at 5 °C afforded colorless crystalline blocks of **7**. Yield: 0.52 g, 41%. M.p. 191–196 °C (decomp.). ^1H NMR ($CDCl_3$, 25 °C): δ (ppm) 0.98–1.11 (m, 12H, $CH(CH_3)_2$), 1.22 (d, 3H, $^1J_{H-H}$ = 6.30 Hz, $CH(CH_3)_2$), 1.38 (s, 6H, C*Me*), 1.67 (d, 9H, $^1J_{H-H}$ = 9.90 Hz, $CH(CH_3)_2$), 1.84 (s, 6H, C*Me*), 2.23 (s, 6H, C*Me*), 2.92 (septet, 2H, $^1J_{H-H}$ = 6.80 Hz, $CH(CH_3)_2$), 7.00–7.17 (m, 6H, H_{aryl}). ^{13}C NMR ($CDCl_3$, 25 °C): δ (ppm) 13.8 (C*Me*), 16.2 (C*Me*), 21.8, 22.2, 22.3, 23.0, 23.4, 23.7, 23.8, 23.8 ($CH(CH_3)_2$), 25.3, 26.8 ($CH(CH_3)_2$), 27.4 (C*Me*), 99.4 (γ-*C*), 121.9, 122.5, 122.9, 124.8 (phenyl C_m), 127.0 128.0 (phenyl C_p), 140.8, 141.1, 141.9, 142.2 (phenyl C_o), 144.9 (phenyl *C*–N), 177.4 (*C*N), 182.4 (*C*O). IR (Nujol Mull): ν (cm^{-1}) 1139 (w), 1561 (m), 3424 (br). MS (*m/z*; (found (Calc.)): 695.2 (695.1) M^+; 553.4 (553.4) M−Cl−^{i}Pr−4Me−3H; 498.3 (498.3) M−Cl−Dipp; 323.9 (322.3) M−Cl−2Dipp−Me; 280.2 (277.3) M−Cl−2Dipp−4Me.

4.8. Synthesis of **8**, [L^2InCl_2]

A −78 °C ether solution of L^2H (0.35 g, 1.8 mmol) had 1 equiv. of *n*-BuLi (1.1 mL of a 1.6 M solution, 1.8 mmol) added drop-wise. After stirring for 2 h at −78 °C, the reaction was allowed to warm to room temperature slowly and stirred overnight. The solvent was then removed and thf added. The thf solution was then added rapidly to a stirred thf suspension of $InCl_3$ (0.39 g, 1.8 mmol) at room temperature. The resulting bright yellow solution was allowed to stir for 12 h, after which time the thf was removed *in vacuo* and the yellow solid extracted into toluene. Concentration of the solution and storage at room temperature afforded **8** as colorless plate crystals. Yield: 0.36 g, 53%. M.p. 201–204 °C. ^1H NMR (C_6D_6, 25 °C): δ (ppm) 0.37 (t, 6H, $^1J_{H-H}$ = 7.20 Hz, CH_3CH_2N), 0.95 (s, 3H, NC*Me*), 1.52 (s, 3H, OC*Me*), 1.70–1.82 (m, 6H, CH_3CH_2N, NCH_2CH_2N), 1.99 (quartet, 2H, $^1J_{H-H}$ = 6.20 Hz, CH_3CH_2N), 4.40 (s, 1H, γ-C*H*). ^{13}C NMR (C_6D_6, 25 °C): δ (ppm) 6.4 (NC*Me*), 21.9 (OC*Me*), 28.8 (CH_3CH_2N), 42.2 (CH_3CH_2N), 48.8 (NCH_2CH_2N), 66.6 (NCH_2CH_2N), 96.4 (γ-CH), 166.7 (*C*N), 187.4 (*C*O). IR (Nujol Mull): ν (cm^{-1}) 942 (m), 1520 (m), 1557 (w), 1577 (w), 3391 (br). MS (*m/z*; (found (Calc.)): 381.4 (382.8) M^+; 199.2 (198.2) $Et_2NCH_2CH_2N(H)C(Me)CHC(Me)O$.

4.9. Synthesis of **9**, [L^1SbCl_3]

A thf solution of L^1Li (0.25 g, 0.90 mmol) was added drop-wise at −78 °C to a stirred thf solution of $SbCl_3$ (0.31 g, 1.3 mmol). The resulting yellow solution was immediately removed from the dry-ice bath and allowed to warm to ambient temperature. Stirring was maintained overnight. Following the removal of thf *in vacuo*,

the pale orange solid was extracted into toluene and filtered. Repeated filtration, concentration, and storage at room temperature for two weeks afforded colorless plate crystals of **9** in moderate yield. Yield: 0.30 g, 67%. M.p. 149–152 °C. ^{1}H NMR ($CDCl_3$, 25 °C): δ (ppm) 1.02–1.23 (m, 12H, CH(CH_3)$_2$), 1.78 (s, 3H, C*Me*), 1.88 (s, 3H, C*Me*), 2.27 (s, 3H, C*Me*), 2.83 (septet, 2H, $^1J_{H-H}$ = 6.80 Hz, C*H*(CH_3)$_2$), 7.14–7.31 (m, 3H, H_{aryl}), 12.84 (s, 1H, N*H*). ^{13}C NMR ($CDCl_3$, 25 °C): δ (ppm) 13.6 (C*Me*), 16.8 (C*Me*), 21.8 (CH(*C*H_3)$_2$), 23.5 (CH(*C*H_3)$_2$), 25.4 (*C*H(CH_3)$_2$), 27.6 (C*Me*), 99.1 (γ-*C*), 122.9 (phenyl C_m), 127.9 (phenyl C_p), 131.7 (phenyl C_o), 144.4 (phenyl *C*–N), 167.7 (*C*N), 189.9 (*C*O). IR (Nujol Mull): ν (cm^{-1}) 1170 (m), 1575 (m), 3185 (shoulder, N–H stretch). MS (*m/z*; (found (Calc.)): 500.4 (501.5) M^+; 380.4 (380.1) M−3Cl−Me; 274.3 (273.4) M−$SbCl_3$.

4.10. Synthesis of **10**, L^2SbCl_2

A −78 °C ether solution of L^2H (1.5 g, 7.5 mmol) had 1 equiv. of *n*-BuLi (3.0 mL of a 2.5 M solution, 7.5 mmol) added drop-wise. After stirring for 2 h at −78 °C, the reaction was allowed to warm to room temperature slowly and stirred overnight. The solvent was then removed and toluene added. The toluene solution was then slowly added by cannula to a stirred suspension of $SbCl_3$ (1.7 g, 7.5 mmol) in a toluene-thf mixture at room temperature. The initial yellow reaction gradually turned dark orange and was allowed to stir overnight. Following the removal of toluene *in vacuo*, the dark orange-red solid was extracted into thf and filtered. Concentration under reduced pressure of the thf solution and storage at −30 °C afforded colorless crystalline chunks of **10**. Yield: 0.55 g, 19%. M.p. 108–112 °C (decomp.). ^{1}H NMR ($CDCl_3$, 25 °C): δ (ppm) 1.25 (t, 6H, $^1J_{H-H}$ = 7.35 Hz, C*H*$_3$CH$_2$N), 1.94 (s, 3H, NC*Me*), 1.96 (s, 3H, OC*Me*), 2.90–2.97 (m, 4H, NCH_2CH_2N), 3.66–3.75 (m, 4H, CH_3CH_2N), 4.97 (s, 1H, γ-C*H*). ^{13}C NMR ($CDCl_3$, 25 °C): δ (ppm) 7.6 (NC*Me*), 18.1 (OC*Me*), 24.6 (*C*H$_3$CH$_2$N), 27.9 (*C*H_3CH$_2$N), 42.9 (CH$_3$*C*H$_2$N), 45.9 (CH$_3$*C*H$_2$N), 50.8 (N*C*H$_2$CH$_2$N), 66.9 (NCH$_2$*C*H$_2$N), 100.9 (γ-*C*H), 161.7 (*C*N), 190.5 (*C*O). IR (Nujol Mull): ν (cm^{-1}) 1521 (m), 1580 (m), 1613 (w). MS (*m/z*; (found (Calc.)): 391.2 (389.9) M^+; 361.4 (360.9) M−Et; 199.2 (198.2) $Et_2NCH_2CH_2N$(H)C(Me)CHC(Me)O.

Acknowledgment

The Robert A. Welch foundation is thanked for financial support.

Appendix A. Supplementary material

CCDC 691684, 691685, 691686, 691687, 691688, 691689, 691690, 691691, 691692 and 691693 contains the supplementary crystallographic data for this paper. These data can be obtained free of charge from The Cambridge Crystallographic Data Centre via www.ccdc.cam.ac.uk/data_request/cif. Supplementary data associated with this article can be found, in the online version, at doi:10.1016/j.jorganchem.2008.07.021.

References

[1] (a) Selected examples include: S.T. Liddle, P.L. Arnold, Dalton Trans. 30 (2007) 3305;
(b) X.-H. Wei, J.D. Farwell, P.B. Hitchcock, M.F. Lappert, Dalton Trans. 8 (2008) 1073;
(c) G. Bai, P. Wei, A. Das, D.W. Stephan, Organometallics 5 (2006) 5870;
(d) Y. Yang, T. Schulz, M. John, A. Ringe, H.W. Roesky, D. Stalke, J. Magull, H. Ye, Inorg. Chem. 47 (2008) 2585;
(e) Z. Lu, M. Findlatter, A.H. Cowley, Chem. Commun. 2 (2008) 184;
(f) S.P. Green, A. Stasch, C. Jones, Science 318 (2007) 1754;
(g) R.E. Cowley, J. Elhaik, N.A. Eckert, W.W. Brennessel, B. Eckard, P.L. Holland, J. Am. Chem. Soc. 130 (2008) 6074;
(h) L. Bourget-Merle, M.F. Lappert, J.R. Severn, Chem. Rev. 102 (2002) 3031.
[2] (a) X.F. Li, K. Dai, W.P. Ye, L. Pan, Y.S. Li, Organometallics 23 (2004) 1223;
(b) D. Zhang, G.X. Jin, L.H. Weng, F.S. Wang, Organometallics 23 (2004) 3270;
(c) B.Y. Liu, C.Y. Tian, L. Zhang, W.D. Yan, W.J. Zhang, J. Polym. Sci. Polym. Chem. 44 (2006) 6243.
[3] (a) A.R. Sadique, W.W. Brennessel, P.L. Holland, Inorg. Chem. 47 (2008) 784;
(b) J. Spielmann, S. Harder, Chem. Eur. J. 13 (2007) 8928;
(c) G. Bai, P. Wei, A.K. Das, D.W. Stephan, Dalton Trans. 9 (2006) 1141;
(d) L.A. MacAdams, G.P. Buffone, C.D. Incarvito, A.L. Rheingold, K.H. Theopold, J. Am. Chem. Soc. 127 (2005) 1082.
[4] N.N. Greenwood, A. Earnshaw, Chemistry of the Elements, second ed.
[5] (a) M. Mazzeo, M. Lamberti, A. Tuzi, R. Centore, C. Pellecchia, Dalton Trans. (2005) 3025;
(b) F. Basuli, B.C. Bailey, J. Tomaszewski, J.C. Huffman, D.J. Mindiola, J. Am. Chem. Soc. 125 (2003) 6052;
(c) D.A. Pennington, D.L. Hughes, M. Bochmann, S.J. Lancaster, Dalton Trans. (2003) 3480.
[6] (a) G.D. Smith, C.N. Caughlan, J.A. Campbell, Inorg. Chem. 11 (1972) 2989;
(b) J.E. Hill, P.E. Fanwick, I.P. Rothwell, Acta Crystallogr. C. C47 (1991) 541.
[7] (a) J.L. Petersen, Inorg. Chem. 19 (1980) 181;
(b) J.C. Galluci, N. Kozima, L.A. Paquette, Acta Crystallogr. C. 54 (1988) 1609;
(c) F. Caruso, M. Rossi, J. Tanski, R. Sartori, R. Sariego, S. Moya, S. Diez, E. Navarrete, A. Cingolani, F. Marchetti, C. Pettinari, J. Med. Chem. 43 (2000) 3665;
(d) G.R. Willey, J. Palin, M.G.B. Drew, J. Chem. Soc., Dalton. Trans. (1994) 1799.
[8] G.M.H. van der Welde, S. Harkema, P.J. Gellings, Inorg. Chim. Acta 11 (1974) 243.
[9] (a) P. Piszczek, M. Richert, A. Wojtczak, Polyhedron 27 (2008) 602;
(b) J. Okuda, E. Herdtweck, Inorg. Chem. 30 (1991) 516.
[10] (a) W.F. Beck, G.W. Brudvig, J. Am. Chem. Soc. 110 (1988) 1517;
(b) K. Wieghardt, Angew Chem., Int. Ed. Engl. 28 (1989) 1153;
(c) W.F. Beyer, I. Fridovich, Biochemistry 24 (1985) 6460.
[11] H. Jacobsen, L. Cavallo, Chem. Eur. J. 7 (2001) 800.
[12] (a) C.-G. Zhang, J. Sun, X.-F. Kong, C.-X. Zhao, J. Chem. Cryst. 29 (1999) 203;
(b) A. Panja, N. Shaikh, M. Ali, P. Vojtisek, P. Banerjee, Polyhedron 22 (2003) 1191;
(c) D. Das, C. Pyeng, C. Cheng, J. Chem. Soc., Dalton Trans. (2000) 1081;
(d) G. Lenoble, P.G. Lacroix, J.C. Daran, S.D. Bella, K. Nakatani, Inorg. Chem. 37 (1998) 2158;
(e) H. Asada, M. Fujiwara, T. Matsushita, Polyhedron 19 (2000) 2039.
[13] (a) N.A. Law, T.E. Machonkin, J.P. McGorman, E.J. Larson, J.W. Kampf, V.L. Pecoraro, J. Chem. Soc., Chem. Commun. (1995) 2015;
(b) Mn–Cl examples:J. Strauch, T.H. Warren, G. Erker, R. Frohlich, P. Saarenketo, Inorg. Chim. Acta 300 (2000) 810;
(c) A.F. Mason, G.W. Coates, J. Am. Chem. Soc. 126 (2004) 16326;
(d) D.A. Pennington, W. Clegg, S.J. Coles, R.W. Harrington, M.B. Hursthouse, D.L. Hughes, M.E. Light, M. Schormann, M. Bochmann, S.J. Lancaster, Dalton Trans. (2005) 561;
(e) R.K.J. Bott, D.L. Hughes, M. Schormann, M. Bochmann, S.J. Lancaster, J. Organomet. Chem. 665 (2003) 135.
[14] (a) S. Wang, H.-W. Li, Z. Xiem, Organometallics 23 (2004) 2469;
(b) N.A. Eckert, J.M. Smith, R.J. Lachicotte, P.L. Holland, Inorg. Chem. 43 (2004) 3306;
(c) S. Langley, M. Helliwell, J. Raftery, E.I. Tolis, R.E.P. Winpenny, Chem Commun. (2004) 142;
(d) P.W. Roesky, Organometallics 21 (2002) 4756.
[15] (a) D. Wang, M. Wang, X. Wang, R. Zhang, J. Ma, L. Sun, J. Mol. Catal. A: Chem. 270 (2007) 278;
(b) A. Panda, M. Stender, R.J. Wright, M.M. Olmstead, P. Klavins, P.P. Power, Inorg. Chem. 41 (2002) 3909.
[16] Q. Su, Q.-L. Wu, G.-H. Li, X.-M. Liu, Y. Mu, Polyhedron 26 (2007) 5053.
[17] (a) N.H. Cromwell, F.A. Miller, A.R. Johnson, R.L. Frank, D.J. Wallace, J. Am. Chem. Soc. 71 (1949) 3337;
(b) H.F. Holtzclaw Jr., J.P. Collman, R.M. Alire, J. Am. Chem. Soc. 80 (1958) 1100;
(c) J.-P. Costes, Polyhedron 6 (1987) 2169.
[18] (a) J. Vekla, L. Zhu, C.J. Flaschenriem, W.W. Brennessel, R.J. Lachicotte, P.L. Holland, Organometallics 26 (2007) 3416;
(b) J. Prust, A. Stasch, W. Zheng, H.W. Roesky, E. Alexopoulos, I. Uson, D. Boehler, T. Schuchardt, Organometallics 20 (2001) 3825;
(c) A.P. Dove, V. Gibson, E.L. Marshall, A.J.P. White, D.J. Williams, Dalton Trans. (2004) 570;
(d) S.D. Allen, D.R. Moore, E.B. Lobovsky, G.W. Coates, J. Organomet. Chem. 683 (2003) 137.
[19] (a) J.D. Farwell, P.B. Hitchcock, M.F. Lappert, G.A. Luintra, A.V. Protechenko, X-H. Wei, J. Organomet. Chem. 693 (2008) 1861;
(b) D.J. Doyle, V.C. Gibson, A.J.P. White, Dalton Trans. (2007) 358;
(c) J. Hunger, S. Blaurock, J. Sieler, Z. Anorg. Allg. Chem. 631 (2005) 472;
(d) S.D. Allen, D.R. Moore, E.B. Lobkovsky, G.W. Coates, J. Organomet. Chem. 683 (2003) 137.
[20] B. Liu, C. Tian, L. Zhang, W. Yan, W. Zhang, J. Polym. Sci. 44 (2006) 6243.
[21] W.-Y. Lee, H.-H. Hsieh, C.-C. Hsieh, H.M. Lee, G.-H. Lee, J.-H. Huang, T.-C. Wu, S.-H. Chuang, J. Organomet. Chem. 692 (2007) 1131.

[22] (a) Z. Lu, G. Reeske, J.A. Moore, A.H. Cowley, Chem. Commun. 48 (2006) 5060;
(b) A.F. Gushwa, A.F. Richards, Eur. J. Inorg. Chem. 5 (2008) 728;
(c) F. Basuli, J.C. Huffmann, D.J. Mindiola, Inorg. Chem. 42 (2003) 8003.
[23] F.H. van der Steen, J. Boersma, A.L. Speak, G. van Koten, Organometallics 10 (1991) 2467.
[24] A. Haaland, Angew. Chem., Int. Ed. Engl. 101 (1989) 1017.
[25] R.L. Geerts, J.C. Huffman, K.G. Caulton, Inorg. Chem. 25 (1986) 590.
[26] X. Pang, X. Chen, X. Zhuang, X. Jing, J. Polym. Sci. Part A: Polym. Chem. 46 (2008) 643.
[27] (a) P.A. van der Schaaf, E. Wissing, J. Boersma, W.J.J. Smeets, A.L. Spek, G. van Koten, Organometallics 12 (1993) 3624;
(b) V. Patroniak, P.N.W. Baxter, J.-M. Lehn, M. Kubicki, M. Nissinen, K. Rissanen, Eur. J. Inorg. Chem. (2003) 4001;
(c) M. Alexiou, E. Katsoulakou, C. Dendrinou-Samara, C.P. Raptopoulou, V. Psycharis, E. Manessi-Zoupa, S.P. Perlepes, D.P. Kessissoglou, Eur. J. Inorg. Chem. (2005) 1964;
(d) R. Murugavel, S. Kuppuswamy, R. Boomishankar, A. Steiner, Angew. Chem., Int. Ed. 45 (2006) 5536.
[28] (a) H.M.M. Shearer, C.B. Spencer, J. Chem. Soc., Chem. Commun. (1996) 194;
(b) H.M.M. Shearer, C.B. Spencer, Acta Crystallogr. Sect. B B36 (1980) 2046;
(c) J.G. Noltes, J.J. Boerma, J. Organomet. Chem. 12 (1968) 425;
(d) M.M. Olmstead, P.P. Power, S.C. Shoner, J. Am. Chem. Soc. 113 (1991) 3379.
[29] Z. He, C. He, Z.-M. Wang, E.-Q. Gao, Y. Liu, C.-H. Yan, Dalton Trans. (2004) 502.
[30] A.L. Spek, Acta Crystallogr. A 46 (1990) 194.
[31] H.E. Gottlieb, V. Kotlyar, A. Nudelman, J. Org. Chem. 62 (1997) 7512.
[32] (a) N. Nimitsiriwat, V.C. Gibson, E.L. Marshall, P. Takolpuckdee, A.K. Tomov, A.J.P. White, D.J. Williams, M.R.J. Elsegood, S.H. Dale, Inorg. Chem. 46 (2007) 9988;
(b) M.L. Cole, D.J. Evans, P.C. Junk, L.M. Louis, New J. Chem. 56 (2002) 1015;
(c) F.A. Cotton, L.M. Daniels, L.R. Falvello, J.H. Matonic, C.A. Murillo, X. Wang, H. Zhou, Inorg. Chim. Acta 266 (1997) 91.
[33] (a) T.-Y. Chou, Y. Chi, S.-F. Huang, C.-S. Liu, A.J. Carty, L. Scoles, K.A. Udachin, Inorg. Chem. 42 (2003) 6041;
(b) D.A. Neumayer, A.H. Cowley, A. Decken, R.A. Jones, V. Lakhotia, J.G. Ekedrt, J. Am. Chem. Soc. 117 (1995) 5893;
(c) R.A. Fischer, H. Sussek, A. Miehr, H. Pritzkow, E. Herdtweck, J. Organomet. Chem. 548 (1997) 73;
(d) J. Kim, S.G. Bott, D.M. Hoffmann, J. Chem. Soc., Dalton Trans. (1999) 141.
[34] (a) J.N. Avaritsiotis, R.P. Howson, Thin Solid Films 80 (1980) 63;
(b) A. Wang, J. Dai, J. Cheng, M.P. Chudzik, T.J. Marks, R.P.H. Chang, C.R. Kannewurf, Appl. Phys. Lett. 73 (1998) 327.
[35] (a) R. Nomura, S. Inazawa, H. Matsuda, S. Saeki, Polyhedron 6 (1987) 507;
(b) T. Maruyama, K.J. Fukui, J. Appl. Phys. 70 (1991) 3848;
(c) S. Reich, H. Suhr, B. Waimer, Thin Solid Films 189 (1990) 293.
[36] (a) J. Lewiński, J. Zachara, K.B. Starowieyski, J. Chem. Soc., Dalton. Trans. (1997) 4217;
(b) J. Lewiński, J. Zachara, T. Kopeć, K.B. Starowieyski, J. Lipowski, I. Justyniak, E. Kolodziejczyk, Eur. J. Inorg. Chem. (2001) 1123;
(c) J. Lewiński, J. Zachara, I. Justyniak, Organometallics 16 (1997) 4597.
[37] T.-Y. Chou, Y. Chi, S.-F. Huang, C.-S. Liu, A.J. Carty, L. Scoles, K.A. Udachin, Inorg. Chem. 42 (2003) 6041.
[38] K. Gilg, P. Klüfers, Acta Crystallogr. E E63 (2007) 4764.
[39] M. Khan, R.C. Steevensz, D.G. Tuck, J.G. Noltes, P.W.R. Corfield, Inorg. Chem. 19 (1980) 3407.
[40] (a) M.S. Hill, P.B. Hitchcock, Chem. Commun. (2004) 1818;
(b) M. Stender, P.P. Power, Polyhedron 21 (2002) 525;
(c) M.S. Hill, P.B. Hitchcock, P. Pongtavornpinyo, Dalton Trans. (2007) 731.
[41] L.A. Lesikar, A.F. Richards, J. Organomet. Chem. 691 (2006) 4250.
[42] (a) F. di Bianca, E. Rivarola, A.L. Spek, H.A. Meinema, J.G. Noltes, J. Organomet. Chem. 63 (1973) 293;
(b) L.E. Turner, M.G. Davidson, M.D. Jones, H. Ott, V.S. Schulz, P.J. Wilson, Inorg. Chem. 45 (2006) 6123.
[43] (a) D. Neculai, H.W. Roesky, A.M. Neculai, J. Magull, H.-G. Schmidt, M. Notemeyer, J. Organomet. Chem. 643–644 (2002) 47;
(b) R.-C. Yu, C.-H. Hung, J.-H. Huang, H.-Y. Lee, J.-T. Chen, Inorg. Chem. 41 (2002) 6450.
[44] G.M. Sheldrick, SHELXS-97, Program for the Solution of Crystal Structures; University of Göttingen, Germany, 1997 and G.M. Sheldrick, SHELXL-97, Program for the Refinement of Crystal Structures.